J. King Saud Univ., Vol. **3**, *Eng. Sci.* (1), pp. 45–57 (1411H/1991)

Steady State Stability of Superconducting Generators

M.A.A.S. Alyan
Electrical Eng. Dept., College of Engineering
King Saud University, P.O. Box 800, Riyadh 11421, Saudi Arabia

Abstract. This paper reports on the results of a simulation study carried out to determine the steady state stability characteristics of superconducting generators. The influence of forcing functions via the excitation system and prime mover have been included in the analysis. The results show that using excitation control augmented with Power System Stabilizers (PSS) provides positive damping and improves the steady state stability of superconducting generators.

List of Symbols

H	=	inertia constant, sec
i	=	current, p.u.
V	=	voltage, p.u.
R	=	resistance, p.u.
X	=	self, mutual reactance, p.u.
T	=	torque, p.u.
ψ	=	flux linkage, p.u.
A,B,C,D,E,F,P,Z,Q	=	matrices
δ	=	rotor angle with respect to infinite bus voltage
$p\delta, \dot{\delta}$	=	rate of change of the rotor angle
$p\omega, p\dot{\delta}$	=	rotor acceleration
ω_0	=	rated angular frequency, rad/sec
T_e	=	electromagnetic torque, p.u.
T_m	=	mechanical torque
τ	=	time constant
ξ	=	damping ratio
$p = d/dt$	=	differential operator
Δ	=	change in quantity

Subscripts

a	=	armature
d,q	=	armature (d–, q–axis)
D1, Q1	=	outer screet (d–, q–axis)
D2, Q2	=	inner secreet (d–, q–axis)
F	=	field winding
t	=	terminal
e	=	external
b	=	bus-bar
0	=	steady state value

Introduction

The application of superconducting technology to turbine-generators has been stimulated by the significant potential advantages of these generators over their conventional counterparts [1–4]. The perceived benefits include higher generator efficiency, reduced physical size and weight, and improved steady state as well as transient performance. Superconducting generators have the potential to break through the rating limits of conventional generators and to generate directly at transmission line voltages. Furthermore, the development of new superconducting materials which can tolerate large variations in the transient magnetic fields and currents has made it feasible to develop machines with superconducting field and armature windings [4]. Such superconductors with enhanced performance capabilities will affect the field winding transient capability and thus will ultimately lead to large base-load units which could maintain a state of superconductivity even during large system disturbances. These new superconducting wires will also permit effective excitation control to be applied without any threat of quenching.

This paper mainly deals with the possibility of improving the damping of rotor oscillations of superconducting generators through the use of supplementary stabilizing signals to the Automatic Voltage Regulator (AVR) loop. Influence of governor control on stability of superconducting generators has been reported elsewhere [5,6]. This possibilities of co-ordinating the exciter and governor effects in an integrated control scheme is also considered in this paper. The generator considered this investigation has a superconducting field winding surrounded with electromagnetic shield and damper screens.

Mathematical Model

A linearized mathematical model of the generator and its associated controllers may be obtained in the state-space form as

$$\dot{X} = AX + BU \tag{1}$$

where X is the state vector, U is the input vector and A and B are the state and input coefficient matrices respectively. The state coefficient matrix A of the system under consideration is obtained by using a direct method as given in the Appendix. The method described is particularly helpful in cases where it is necessary to represent any of the eddy current screens by multi-layers on each axis or when it is required to adequately represent the eddy currents in solid iron rotors of conventional turbine-generators by multi-rotor circuits on each axis.

System Description

The system considered consists of a superconducting turbine-generators unit connected to an infinite bus by a transformer and a tie line. The unit is equipped with thyristor exciter, AVR, PSS, and electro hydraulic governor. The alternator is represented by a ninth-order model based on Park's equations [5]. Since the present study is concerned with low-frequency oscillations, it is adequate to represent each screen by one coil of fixed parameters on each axis. The parameter values of the generator are given in Table 1 [6]. These parameters were computed by using a three-dimensional field model.

Table 1. Parameters of superconducting generator [6] reactance in p.u.

MVA	2000
Rated power (MW)	1700
$X_d = X_q$	0.545
$X_{D1} = X_{Q1}$	0.257
$X_{D2} = X_{Q2}$	0.423
X_F	0.541
$X_{dF} = X_{dD1} = X_{dD2} = X_{FD1} = X_{D1D2}$	0.237
X_{FD2}	0.39
$X_{qQ1} = X_{qQ2} = X_{Q1Q2}$	0.237
R_a	0.003
Outer Screen time constant, sec	0.081
Inner Screen time constant, sec	1.0
Field winding time constant, sec	750
H (KW.Sec/KVA)	3

Transformer and transmission line impedance 0.008 + j 0.2

The excitation system considered is a fast acting thyristor exciter with a negligible time lag. An automatic voltage regulator is used with the exciter to control the generator terminal voltage. The PSS considered is a speed stabilizer applied to the voltage regulator loop. A signal from the speed is applied through a lead/lag compensating network to the reference of the voltage regulator. Studies [7,8] have shown that this is a very effective stabilizer for conventional synchronous machines. The same stabilizer structure has been used for the superconducting generator in the present paper. The block diagram of the stabilizer is shown in Fig. 1a. Selection of PSS parameters is based upon eigenvalue analysis to achieve satisfactory improvement in damping.

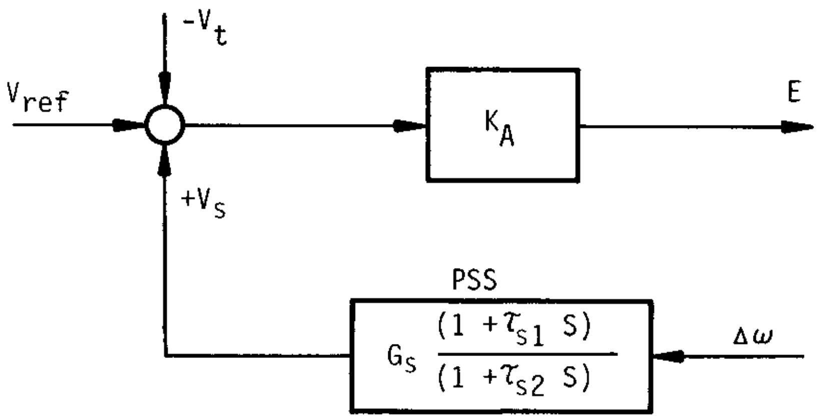

(a) AVR and PSS model

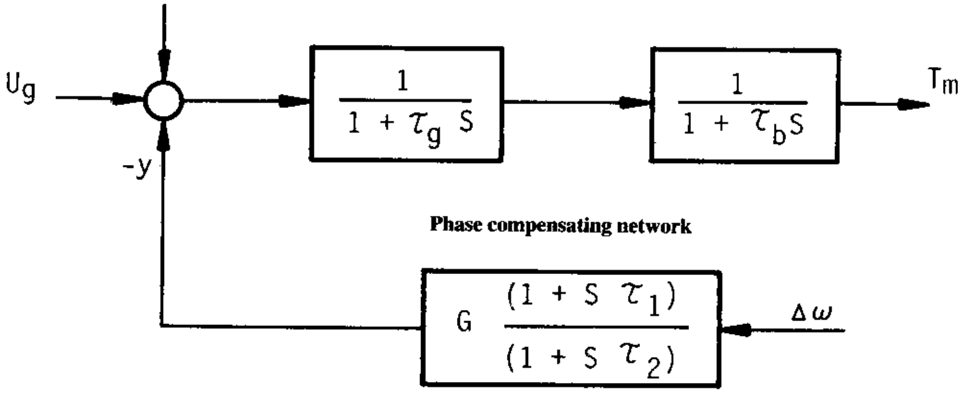

(b) Governer and turbine model

Fig. 1.Schematic diagram of the control system

The block diagram of the governor and turbine system considered is shown in Fig. 1b. Both the governor and the turbine is represented by a first order transfer function. This representation has been adequate for steady state stability studies. A phase advance network (Fig. 1b) is incorporated in the governor feedback loop.

Results and Discussion

It is assumed that the generator is delivering full load at 0.85 power factor lagging at rated terminals voltage. The stabilizing signal from PSS is applied to the AVR reference point. The eigenvalues of the system coefficient matrix are computed by means of a standard algorithm. The influence of AVR and PSS parameters on the critical eigenvalues of rotor oscillations is examined. The results are given in Fig. 2. This Figure shows considerable improvement in the damping of rotor oscillations (the negative real part of the critical eigenvalues) with an increase in the AVR and PSS parameters, τ_{s2} is kept constant at a value of 0.01 sec. The damping ratio is computed and plotted in Fig. 3. This Figure shows an increase in ξ reaching about 0.2. The value of gains and time constant to achieve this value are much higher than the values normally used for conventional synchronous machines. This is due to the extremely long time constant of superconducting field windings. The other eigen modes show no serious sacrifice in system performance.

Governor Control

In this section only governor control is considered while the exciter control is inoperative. The eigenvalues are computed as before. Fig. 4 shows the effect of increasing the time constant of the phase compensating network incorporated in the governor feedback loop. The Figure shows an improvement in damping with increase in the time constant. The results are in agreement with reference [5,6].

Co-ordinated Control system

Co-ordinating the control efforts of the exciter and governor in an integrated system is considered in this section.The combined effect of the two controlling schemes is included in the model. The parameters of the governor loop is kept constant, while the AVR and PSS gains are varied. The results of damping ratio for this case are shown by the dotted curves in Fig. 3. These indicate that at low values of AVR and PSS gains, the damping is contributed by governor action. The damping ratio increases with increase of these gains due to the contribution of the PSS action until it reaches the value obtained with excitation control acting alone at the intersection point of the two curves. Limited improvement in damping ratio is obtained beyond this point although the damping α is increasing. This is due to the increase in frequency of oscillation which increases the damping ratio.

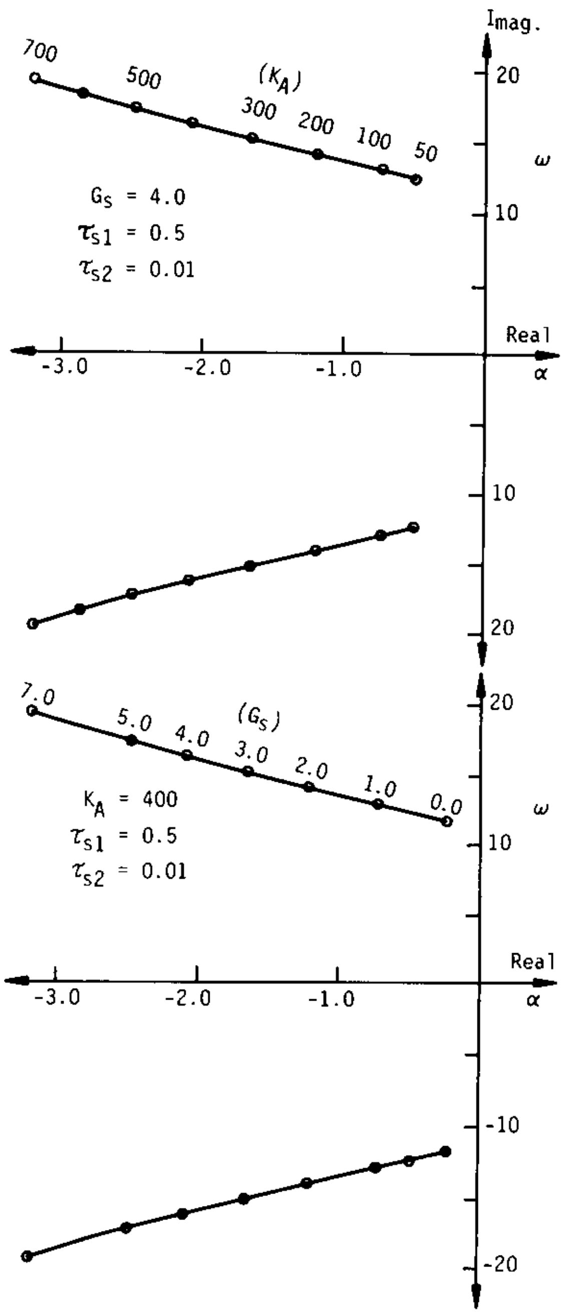

Fig. 2. Variation of critical eigenvalues with AVR and PSS gaines

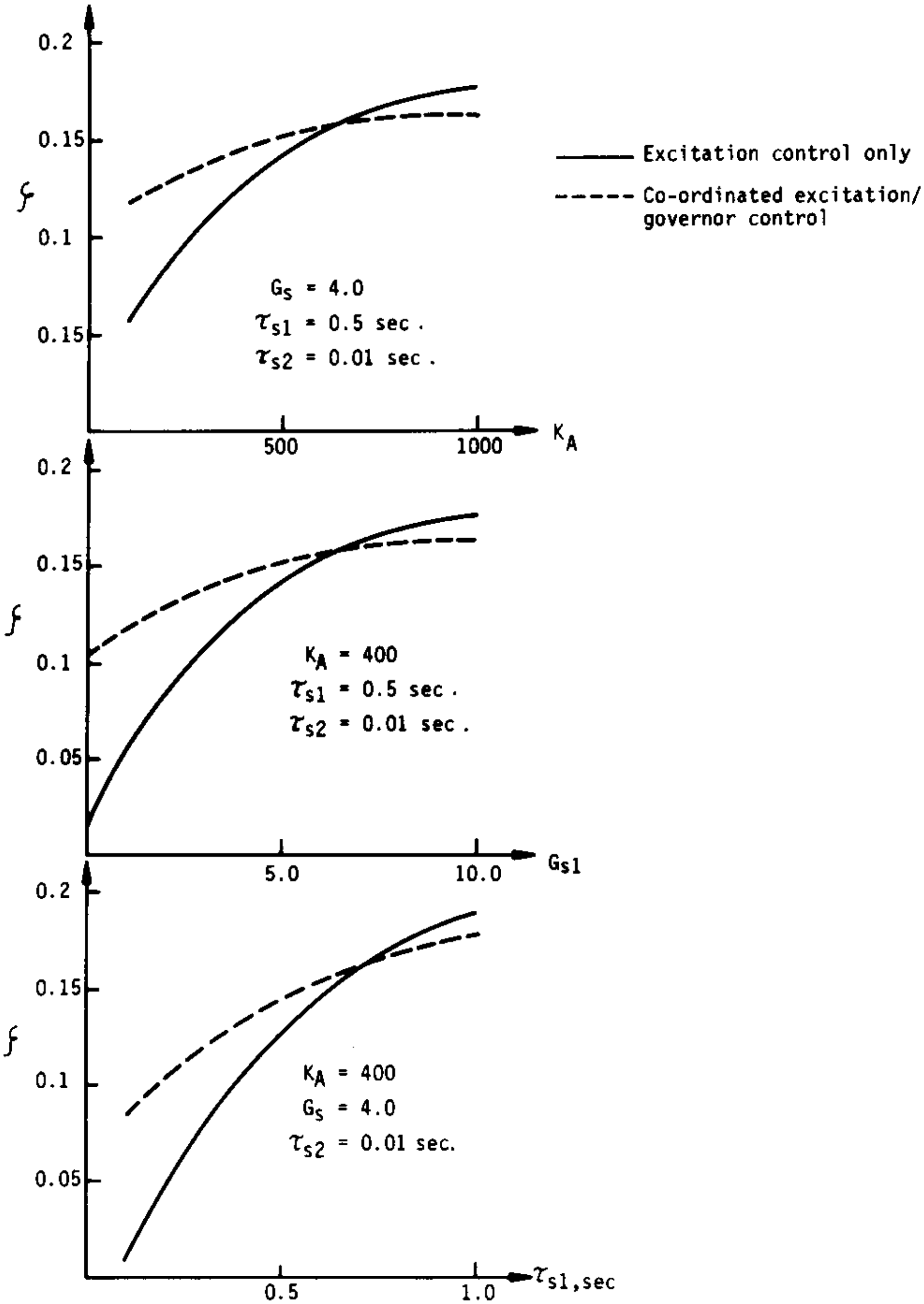

Fig. 3. Variation of damping ratio wth AVR and PSS parameters

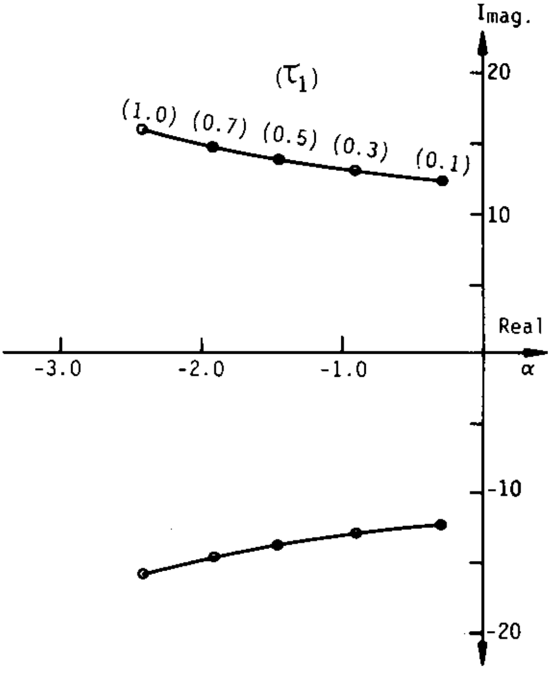

(a) Variation of critical eigenvalues

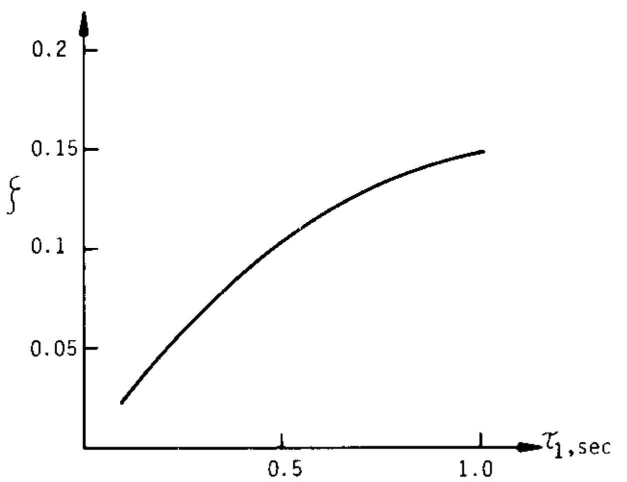

(b) Variation of damping ratio

Fig. 4. Variation of critical eigenvalues and damping ratio with phase compensating network time constant

Table 2. Governor and turbine parameters

Governor time constant τ_g, sec.	0.1
Turbine time constant τ_b, sec.	0.3
Phase compensating network time consants	
τ_1, sec	0.5
τ_2, sec	0.01

Conclusions

The main aspect of steady state stability of superconducting generators with excitation and/or governor control is outlined in this study. Additional positive damping could be achieved by using a supplementary stabilizing signal derived from speed to the AVR reference point. The order of AVR and PSS parameters to achieve satisfactory improvement in damping is determined. The parameters are much higher than those used for conventional synchronous machines. Co-ordination between the exciter and governor efforts is possible. Such a co-ordination offers benefits in the lower range of parameters. However, such benefits cease to exist as the parameter values are increased.

References

[1]. Keim, T.A.; Laskaris, T.E.; Fealey, J.A. and Rios, P.A. "Design and Manufacture of a 20 MVA Superconducting Generator". *IEEE Trans.*, PAS-104, No.6 (1985), 1475-1483.

[2]. Fealey, J.E.; Jones, W.D.; Keim, T.A. and Laskaris, T.E. "Comprehensive Test and Evaluation of a 20 MVA Superconducting Generator". *IEEE Trans.*, PAS-104, No.6 (1985), 1484-1491.

[3]. Nathenson, R.D.; Cherepko, J. and Patel, M.R. "Thermal Stress Analysis and Design of the Stator of a 300-MVA Superconducting Generator". *IEEE Trans.*, EC-1, No.3 (1986), 141-147.

[4]. Brunet, Y.; Saberie, J.L. and Tixador, F. "Electrical Design of Air-Cored Synchronous Generators Using Superconducting Field and Armature Windings". *IEE Proc.*, 134, pt. B, No. 1 (1987), 47-52.

[5]. Alyan, M.A.A.S. "Transient Performance of a Superconducting Turbo-Alternator with Governor Control". *J. Eng. Sci.* King Saud University, 12, No.1 (1986), 83-98.

[6]. Alyan, M.A.A.S. and Rahim, Y.H.A. "The Role of Governor Control in Transient Stability of Superconducting Turbo-Generators". *IEEE Trans.* EC-2, No.1, (1987), 38-46.

[7]. deMello, F.P. and Concordia, C.C. "Concepts of Synchronous Machine Stability as Affected by Excitation Control". *IEEE Trans.* PAS-88 (1969), 316-324.

[8]. Busby, E.L.; Hurley, J.D.; Keay, F.W. and Raczkowski, C. "Dynamic Stability Improvement at Monticells Station-Analytical Study and Field Tests". *IEEE Trans.* PAS-98 (1979), 889-901.

Appendix

Linearized Equations of the Generator

The linearized Park's equations of a superconducting generator connected to an infinite bus are given as [5]:

$$\Delta\dot{\psi}_F = -\omega_0 R_F + \Delta i_F + \omega_0 \frac{R_F}{X_{dF}} \Delta E \tag{2}$$

$$\Delta\dot{\psi}_d = \omega_0 \Delta\psi_q + \psi_0 (R_a + R_e) \Delta i_d + \omega_{q0} \Delta\omega + \omega_0 \Delta V_{db} \tag{3}$$

$$\Delta\dot{\psi}_{D1} = -\omega_0 R_{D1} \Delta i_{D1} \tag{4}$$

$$\Delta\dot{\psi}_{D2} = -\omega_0 R_{D2} \Delta i_{D2} \tag{5}$$

$$\Delta\dot{\psi}_q = -\omega_0 \Delta\psi_d + \omega_0 (R_a + R_e) \Delta i_q - \psi_{d0} \Delta\omega + \omega_0 \Delta V_{qb} \tag{6}$$

$$\Delta\dot{\psi}_{Q1} = -\omega_0 R_{Q1} \Delta i_{Q1} \tag{7}$$

$$\Delta\dot{\psi}_{Q2} = -\omega_0 R_{Q2} \Delta i_{Q2} \tag{8}$$

$$\Delta\dot{\omega} = (\Delta T_m - \Delta T_e)\, \omega_0/2H \tag{9}$$

$$\Delta\dot{\delta} = \Delta\omega \tag{10}$$

The various flux linkages are related to the currents as follows:

$$\begin{bmatrix} \Delta\dot{\psi}_F \\ \Delta\dot{\psi}_d \\ \Delta\dot{\psi}_{D1} \\ \Delta\dot{\psi}_{D2} \\ \Delta\dot{\psi}_q \\ \Delta\dot{\psi}_{Q1} \\ \Delta\dot{\psi}_{Q2} \end{bmatrix} = \begin{bmatrix} X_F & -X_{dF} & X_{FD1} & X_{FD2} & & & \\ X_{dF} & -(X_d + X_e) & D_{dD1} & X_{dD2} & & & \\ X_{FD1} & -X_{dD1} & X_{D1} & X_{D1D2} & & & \\ X_{FD2} & -X_{dD2} & X_{D1D2} & X_{D2} & & & \\ & & & & -(X_q + X_e) & X_{qQ1} & X_{qQ2} \\ & & & & -X_{qQ1} & X_{Q1} & X_{Q1Q2} \\ & & & & -X_{qQ2} & X_{Q1Q2} & X_{Q2} \end{bmatrix} \begin{bmatrix} \Delta i_F \\ \Delta i_d \\ \Delta i_{D1} \\ \Delta i_{D2} \\ \Delta i_q \\ \Delta i_{Q1} \\ \Delta i_{Q2} \end{bmatrix} \tag{11}$$

where

$$\Delta V_{db} = V_b \cos\delta . \Delta\delta$$

$$\Delta V_{qb} = -V_b \sin\delta . \Delta\delta$$

$$\triangle T_e = i_q \triangle \psi_d - i_d \triangle \psi_q - \psi_q \triangle i_d + \psi_d \triangle i_q$$

For tie line and Transformer the equations are

$$\triangle V_{dt} = V_b \cos\delta . \triangle\delta + R_e \triangle i_d - X_e \triangle i_q \quad (12)$$

$$\triangle V_{qt} = -V_b \operatorname{Sin}\delta \triangle\delta + X_e \triangle i_d + R_e \triangle i_q \quad (13)$$

$$\triangle V_t = \frac{V_{dt}}{V_t} \triangle V_{dt} + \frac{V_{qt}}{V_t} \triangle V_{qt} \quad (14)$$

Equations (2) to (10) may be arranged in matrix form as given in equation (24) at the end of the appendix and can be written as follows:

$$\dot{X} = CX + D\triangle i + BU \quad (15)$$

The state coefficient matrix A may be obtained by multiplying the matrix D by the inverse of the p.u. machine inductance matrix given by equation (11). The product of the multiplication is added to the matrix C in order to obtain the matrix A.

Excitation System

The voltage regulator is considered by introduction of equations (12) and (13), which may be arranged in the matrix form as:

$$\begin{bmatrix} \triangle V_{dt} \\ \triangle V_{qt} \end{bmatrix} = \begin{bmatrix} R_e & -X_e \\ X_e & R_e \end{bmatrix} \begin{bmatrix} \triangle i_d \\ \triangle i_q \end{bmatrix} + \begin{bmatrix} V_b \cos\delta \\ V_b \operatorname{Sin}\delta \end{bmatrix} \begin{bmatrix} \triangle\delta \end{bmatrix}$$

$$\triangle V_{dq} = Z \triangle i + P \triangle\delta \quad (16)$$

equation (14) may be written as

$$\triangle V_t = \begin{bmatrix} \frac{V_{dt}}{V_t} & \frac{V_{qt}}{V_t} \end{bmatrix} \begin{bmatrix} \triangle V_{dt} \\ \triangle V_{qt} \end{bmatrix}$$

or compactly

$$\triangle V_t = E \triangle V_{dq} \quad (17)$$

The substitution of equation (16) in equation (17) gives

$$\triangle V_t = F \triangle i + Q \triangle \delta \quad (18)$$

where

$$F = EZ ; Q = EP$$

$$\triangle E = K_A (-\triangle V_t + \frac{G_s \tau_{s1}}{\tau_{s2}} \triangle\omega + \triangle X_{10}) \tag{19}$$

$$\triangle \dot{X}_{10} = \frac{\triangle X_{10}}{\tau_{s2}} + \frac{G_s}{\tau_{s2}} (1 - \frac{\tau_{s1}}{\tau_{s2}}) \triangle\omega \tag{20}$$

for governor and turbine the equations are

$$\triangle \dot{G}_v = -\frac{1}{\tau_g} \triangle G_v - \frac{1}{\tau_g} \triangle X_{13} - \frac{G\tau_1}{\omega\tau_g\tau_2} \triangle\omega \tag{21}$$

$$\triangle \dot{T}_m = \frac{1}{\tau_g} \triangle G_v - \frac{1}{\tau_b} \triangle T_m \tag{22}$$

$$\triangle \dot{X}_{13} = -\frac{1}{\tau_2} \triangle X_{13} + \frac{G}{\omega\tau_2} (1 - \frac{\tau_1}{\tau_2}) \triangle\omega \tag{23}$$

The expansion of equation (15) is as follows:

$$
\begin{bmatrix} \Delta\dot{\psi}_F \\ \Delta\dot{\psi}_d \\ \Delta\dot{\psi}_{D1} \\ \Delta\dot{\psi}_{D2} \\ \Delta\dot{\psi}_q \\ \Delta\dot{\psi}_{Q1} \\ \Delta\dot{\psi}_{Q2} \\ \Delta\dot{\delta} \\ \Delta\dot{\omega} \end{bmatrix}
=
\begin{bmatrix}
0 & 0 & 0 & 0 & 0 & 0 & 0 & 0 & 0 \\
0 & 0 & 0 & 0 & \omega_0 & 0 & 0 & P_1 & \psi_{q0} \\
0 & 0 & 0 & 0 & 0 & 0 & 0 & 0 & 0 \\
0 & 0 & 0 & 0 & 0 & 0 & 0 & 0 & 0 \\
0 & \omega_0 & 0 & 0 & 0 & 0 & 0 & -P_2 & \psi_{d0} \\
0 & 0 & 0 & 0 & 0 & 0 & 0 & 0 & 0 \\
0 & 0 & 0 & 0 & 0 & 0 & 0 & 0 & 0 \\
0 & 0 & 0 & 0 & 0 & 0 & 0 & 0 & 0 \\
0 & \frac{-\omega_0 i_{q0}}{2H} & 0 & 0 & \frac{\omega_0 i_{d0}}{2H} & 0 & 0 & 0 & 0
\end{bmatrix}
\begin{bmatrix} \Delta\psi_F \\ \Delta\psi_d \\ \Delta\psi_{D1} \\ \Delta\psi_{D2} \\ \Delta\psi_q \\ \Delta\psi_{Q1} \\ \Delta\psi_{Q2} \\ \Delta\delta \\ \Delta\omega \end{bmatrix}
\begin{bmatrix}
-\omega_0 R_F & 0 & 0 & 0 & 0 & 0 & 0 \\
0 & \omega_0(R_a+R_e) & 0 & 0 & 0 & 0 & 0 \\
0 & 0 & -\omega_0 R_{D1} & 0 & 0 & 0 & 0 \\
0 & 0 & 0 & -\omega_0 R_{D2} & 0 & 0 & 0 \\
0 & 0 & 0 & & \omega_0(R_a+R_e) & 0 & 0 \\
0 & 0 & 0 & 0 & 0 & -\omega_0 R_{Q1} & 0 \\
0 & 0 & 0 & 0 & 0 & 0 & -\omega_0 R_{Q2} \\
0 & 0 & 0 & 0 & 0 & 0 & \\
0 & \frac{\omega_0 \psi_{q0}}{2H} & 0 & 0 & \frac{-\omega_0 \psi_{d0}}{2H} & 0 & 0
\end{bmatrix}
\begin{bmatrix} \Delta i_F \\ \Delta i_d \\ \Delta i_{D1} \\ \Delta i_{D2} \\ \Delta i_q \\ \Delta i_{Q1} \\ \Delta i_{Q2} \end{bmatrix}
\begin{bmatrix}
\frac{\omega_0 R_F}{X_{dF}} & 0 \\
0 & 0 \\
0 & 0 \\
0 & 0 \\
0 & 0 \\
0 & 0 \\
0 & \frac{\omega_0}{2H}
\end{bmatrix}
\begin{bmatrix} \Delta E \\ \Delta T_m \end{bmatrix}
$$

$$
P_1 = \omega V_b \, \text{Cos}\delta
$$
$$
P_2 = \omega V_b \, \text{Sin}\delta \qquad (24)
$$

اتزان المولدات ذات التوصيل الفائق

موسى عبدالعزيز سليمان عليان

أستاذ مشارك، قسم الهندسة الكهربائية، كلية الهندسة، جامعة الملك سعود،

ص.ب ٨٠٠، الرياض ١١٤٢١، المملكة العربية السعودية

ملخص البحث. تتناول الورقة دراسة موضوع خواص اتزان المولدات ذات التوصيل الفائق. الدراسة تشمل أيضا تأثير التحكم بواسطة ملفات الحث والمحرك الميكانيكي. تظهر الدراسة أن استخدام التحكم بواسطة ملفات الحث مدعمة بـ«موازن أنظمة القدرة الكهربائية» تزيد من اضمحلال الاهتزازات الصغيرة وتحسن من اتزان المولدات ذات التوصيل الفائق.